Energy Efficiency Analysis of Power Allocation on D-MIMO with Dynamic TDD

Matheus D. Carneiro, Igor M. Guerreiro, Yuri C. B. Silva,
Samuel S. Silva, Victor F. Monteiro, and Abraão de C. Albuquerque

***Abstract*— Distributed multi-input multi-output (D-MIMO) has been proposed for the 6th generation (6G) of mobile communications to provide more uniform networks by connecting each user equipment (UE) to more than one access point (AP) through the same bandwidth resource. To meet the individual traffic demands of each UE in a D-MIMO setup, the use of dynamic time division duplex (D-TDD) has also been considered in the literature, by setting the configuration of the system frame in a user-centric way and considering the user necessity at a given moment, differently from static time division duplex (S-TDD). However, this dynamic approach introduces cross-link interference (CLI) due to the simultaneous coexistence of UEs in uplink (UL) and downlink (DL) in a same network. To deal with CLI and energy efficiency (EE) aspects, this work analyzes a classic power allocation algorithm, known as UL fractional power control (FPC), in the case of D-MIMO systems with D-TDD. The results are presented in terms of the spectral efficiency (SE) and EE performance under such scenarios, indicating that the use of FPC can contribute to implement sustainable networks.**

***Keywords*— D-MIMO, Dynamic TDD, Power Control, Energy Efficiency.**

I. Introduction

For the upcoming 6th generation (6G), the distributed multi-input multi-output (D-MIMO) setup has been proposed, in which each user equipment (UE) is served jointly and coherently by multiple access points (APs) (which form a cluster) in the same geographical area at the same time, using the same bandwidth resource. All APs are controlled, via fronthaul links, by a central processing unit (CPU), which performs Radio Resource Management (RRM). As a result, the system achieves a more uniform system performance along the coverage area, mitigating the edge effect of cellular setup, where the UEs near cell edges suffer from interference and path loss (PL) effect [1].

To meet the individual traffic demands of each UE, a dynamic time division duplex (D-TDD) approach has been proposed. Differently from the usual static time division duplex (S-TDD), in which the system demands define the transmission direction of each time resource, in this new setup, each UE sets its own transmission direction in a user-centric way. As described in [2], usually, in S-TDD setup, the signal has the following components: desired signal, UE-to-AP or AP-to-UE (according to transmission mode) interference, and noise. However, D-TDD introduces cross-link interference (CLI): inter-AP interference (IAI) in uplink (UL), caused by downlink (DL) APs to the UE's receiving cluster, and inter-UE interference (IUI) in DL, caused by UL UEs and experienced at the receiving DL UE. This effect is exemplified in Fig. 1.

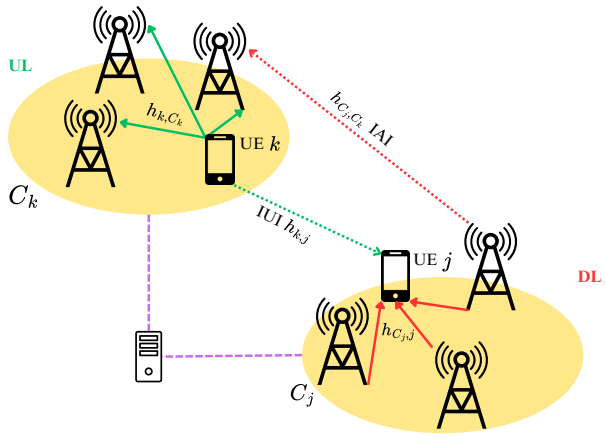

Fig. 1. D-MIMO setup with D-TDD in which two disjoint clusters in different transmit modes suffer from CLI.

In light of this, techniques for mitigating CLI are necessary. In [3], the high-speed fronthaul links connecting the APs are used to suppress and partially cancel the IAI. Additionally, [2] proposes a grouping algorithm to aggregate nearby clusters in the same transmission mode.

Furthermore, power control is a key technique not only for dealing with interference, but also for improving the energy efficiency (EE) of the system. The work in [4] proposes a joint optimization of the power control and the switching point of the transmission direction for each UE via successive convex approximation to improve the EE.

Classic power control approaches, such as fractional power control (FPC), can also be used. For instance, [5] utilizes an FPC algorithm in a cellular scenario with D-TDD. This algorithm is widely explored in the literature with the objective to partially compensate the large scale fading (LSF) effect. Its formulation and operation are described in [6].

In this work, we propose a D-MIMO scenario with D-TDD, following the setup of [2], and the FPC algorithm is implemented to evaluate its effect on the spectral efficiency (SE) and EE for different UL-DL proportions. The results show an improvement in EE through the use of FPC despite a loss in

Matheus D. Carneiro, Igor M. Guerreiro, Yuri C. B. Silva, Samuel S. Silva, Victor F. Monteiro, and Abraão de C. Albuquerque are with the Wireless Telecom Research Group (GTEL), Federal University of Ceará (UFC), Fortaleza, Brazil. E-mails: {matheus.carneiro, igor, yuri, samuelserejo, victor, abraaoalbuquerque}@gtel.ufc.br. This work was supported in part by Brasil 6G project (01245.010604/2020-14, RNP and MCTI), in part by CNPq, in part by FUNCAP/Universal Grant UNI-0210-00043.01.00/23, in part by CAPES. The work of Victor F. Monteiro was supported by CNPq under Grant 308267/2022-2.

terms of SE.

As for the paper organization, section II introduces the system model, detailing the scenario, propagation, and signal models, along with the key performance indicators (KPIs) used for performance evaluation. Section III details the implementation of the power control algorithm in this study. Section IV shows simulation parameters and numerical results. Finally, section V concludes the paper with a summary of the results and their significance.

Notation: In this paper, the following notation is used. Lowercase bold letters (e.g., $\mathbf{h}$) denote vectors; uppercase bold letters (e.g., $\mathbf{H}$) denote matrices and non-bold letters (e.g., h) denote scalars. $(\cdot)^T$ stands for transpose and $|\cdot|$ for modulus of a complex number. $\mathbf{h} \in \mathcal{A}^{N\times 1}$ means this vector belongs to the set $\mathcal{A}$ and has dimension $N \times 1$. Similar notation applies to scalars and matrices. The sets of real numbers and complex numbers are denoted, respectively, by $\mathbb{R}$ and $\mathbb{C}$. $\mathcal{N}(\mu, \sigma^2)$ denotes a real Normal (Gaussian) distribution with mean μ and variance σ^2. $\mathcal{CN}(\mu, \sigma^2)$ denotes a circularly symmetric complex Normal (Gaussian) distribution with mean μ and variance σ^2. $\mathcal{U}(a, b)$ denotes a continuous Uniform distribution over the interval $[a, b]$.

II. System Model

This section presents the system model, including the propagation model, the signal model and the KPIs evaluated.

In this work, we consider a D-MIMO scenario with K single-antenna UEs and M single-antenna APs with a uniform random placement within a square area of side length L and connected to a CPU via fronthaul links. All UEs simultaneously access the same frequency band for both UL and DL transmissions.

As shown in Fig. 1, each UE k is jointly and coherently served by a cluster $\mathcal{C}_k$. This cluster consists of the N APs, from the set of M APs uniformly distributed in the area, that have the strongest LSF $\beta_{k,m}$ to k. This selection is done in the system in such a way that each AP serves only one UE and the clusters are mutually disjoint.

We considered a D-TDD setup, enabling each UE to dynamically transmit or receive according to its needs in each time resource [2].

A. Propagation Model

This subsection explains the system propagation model. For the sake of simplicity, the PL effect $PL_{k,m} \in \mathbb{R}$ (in dB) between a node k and a node m is modeled independently on the link type (UE-UE, UE-AP or AP-AP). The PL equation considers the distance $d_{k,m}$ between the nodes following [1]:

$$PL_{k,m} = -30.5 - 36.7 \log(d_{k,m}[\text{in m}]). \tag{1}$$

The shadowing effect is given by $\eta_{sh} \sim \mathcal{N}(0, \sigma_{sh}^2) \in \mathbb{R}$, where σ_{sh}^2 is the shadowing variance. LSF considers both effects:

$$\beta_{k,m} = 10^{(PL_{k,m}+\eta_{sh})/10}. \tag{2}$$

Furthermore, following [7], each link between two APs and between an AP and a UE can be line-of-sight (LoS) or non line-of-sight (NLoS), taking into account the distance d (in kilometers) between the nodes as follows:

$$\begin{aligned}\text{Prob}_{\text{LoS}}(d) = {} & 0.5 - \min\left(0.5,\, 5\exp\left(-0.156/d\right)\right) \\ & + \min\left(0.5,\, 5\exp\left(-d/0.03\right)\right).\end{aligned} \tag{3}$$

For each link, a random threshold $U \sim \mathbb{U}(0, 1)$ is drawn; the link is considered LoS if $\text{Prob}_{\text{LoS}}(d) > U$. For LoS links, the Rician factor $\overline{K}_{k,m} \sim \mathcal{N}(\mu_k, \sigma_k^2) \in \mathbb{R}$ is applied, otherwise the Rician factor is set to 0, according to [8].

Finally, we adopt the channel model presented in [9]. In the mentioned work, the channel coefficients for UE-UE links are given by $h_{k,k'} = \beta_{k,k'}\, w_{k,k'}$, in which $w_{k,k'} \sim \mathcal{CN}(0, 1) \in \mathbb{C}$ is a Rayleigh scatter distribution that represents the small scale fading (SSF) effect. In contrast, the AP-AP and UE-AP links have Rician channel coefficients, which take into account $\overline{K}_{k,m}$ as follows:

$$h_{k,m} = \left[\sqrt{\frac{\overline{K}_{k,m}}{\overline{K}_{k,m}+1}} + \sqrt{\frac{1}{\overline{K}_{k,m}+1}} w_{k,m}\right] \beta_{k,m}. \tag{4}$$

B. Signal Model

This subsection describes how the signal is modeled for both UL and DL, the signal-to-interference-plus-noise ratio (SINR) and SE considering what is presented in [2].

The UL signal model considers an UE k in UL transmitting the normalized transmit signal x_k to its cluster $\mathcal{C}_k$ with transmit power p_k and channel vector $\mathbf{h}_{\mathcal{C}_k,k} \in \mathbb{C}^{N\times 1}$, in which each element is the channel coefficient of the link between UE k and each AP of $\mathcal{C}_k$. The same is considered for each interfering UL UE j.

Moreover, for interfering APs transmitting the normalized signal s_j, $\mathbf{H}_{\mathcal{C}_k,\mathcal{C}_j} \in \mathbb{C}^{N\times N}$ is denoted as the matrix of channel coefficients between each AP of $\mathcal{C}_k$ and each AP of $\mathcal{C}_j$. $\mathbf{P}_{\mathcal{C}_j} \in \mathbb{R}^{N\times N}$ is a diagonal matrix that contains the square root of the transmit power of each AP of $\mathcal{C}_j$ in the main diagonal. Moreover, $\mathbf{w}_j \in \mathbb{C}^{N\times 1}$ is the transmit beamforming vector of $\mathcal{C}_j$.

Finally, L_j defines the transmission direction by setting 0 for UL and 1 for DL, and $\mathbf{z}_k$ is the UL noise vector. The UL signal is modeled as follows:

$$\begin{aligned}\mathbf{y}_k^{UL} = {} & \underbrace{\sqrt{p_k}\ \mathbf{h}_{\mathcal{C}_k,k}\ x_k}_{\text{desired signal}} + \sum_{\substack{j=1\\ j\neq k}}^{K} \Big(\underbrace{\sqrt{p_j}(1-L_j)\ \mathbf{h}_{\mathcal{C}_k,j}\ x_j}_{\text{UE-to-AP interference}} \\ & + \underbrace{\mathbf{H}_{\mathcal{C}_k,\mathcal{C}_j}\ \mathbf{P}_{\mathcal{C}_j} L_j \mathbf{w}_j\ s_j}_{\text{AP-to-AP interference}} \Big) + \underbrace{\mathbf{z}_k}_{\text{noise}}.\end{aligned} \tag{5}$$

SE is modeled as the logarithm of the sum between 1 and SINR. Then, SE of k-th transmitting user considering a receive beamforming processing $\mathbf{u}_k \in \mathbb{C}^{N\times 1}$ for $\mathcal{C}_k$ is represented as:

$$R_k^{UL} = \log_2\left(1 + \frac{p_k \left|\mathbf{u}_k^T \mathbf{h}_{\mathcal{C}_k,k}\right|^2}{\gamma_k^{UL}}\right), \tag{6}$$

in which γ_k^{UL} aggregates the UE-to-AP interference, IAI and the noise:

$$\gamma_k^{UL} = \sum_{\substack{j=1 \\ j\neq k}}^{K} p_j(1-L_j)\left|\mathbf{u}_k^T \mathbf{h}_{\mathcal{C}_k,j}\right|^2 + L_j\left|\mathbf{u}_k^T\, \mathbf{H}_{\mathcal{C}_k,\mathcal{C}_j}\mathbf{P}_{\mathcal{C}_j}\mathbf{w}_j\right|^2 + \sigma_{\text{UL}}^2\,, \tag{7}$$

where σ_{UL}^2 represents the UL noise variance.

Finally for the UL, the EE considers the ratio between the sum SE of all UEs and the sum of their corresponding transmit powers. It is defined as follows:

$$EE^{UL} = \frac{\sum_{j=1}^{K}(1-L_j)R_k^{UL}}{\sum_{j=1}^{K}(1-L_j)p_k}. \tag{8}$$

For the DL signal, the equation of the signal received by UE k is similar to UL, considers a similar notation and is represented with the specific indexes for this case as follows:

$$y_k^{DL} = \underbrace{\mathbf{h}_{\mathcal{C}_k,k}^T\left(\mathbf{P}_{\mathcal{C}_k}\mathbf{w}_k\right)x_k}_{\text{desired signal}} + \sum_{\substack{j=1 \\ j\neq k}}^{K}\underbrace{\mathbf{h}_{\mathcal{C}_j,k}^T\left(\mathbf{P}_{\mathcal{C}_j}L_j\mathbf{w}_j\right)x_j}_{\text{AP-to-UE interference}} + \underbrace{\sqrt{p_j}(1-L_j)h_{j,k}s_j}_{\text{UE-to-UE interference}} + \underbrace{z_k}_{\text{noise}}. \tag{9}$$

Likewise, the SE of the k-th receiving UE also considers the SINR of DL links and is given by:

$$R_k^{DL} = \log_2\left(1 + \frac{|\mathbf{h}_{\mathcal{C}_k,k}^T\ (\mathbf{P}_{\mathcal{C}_k}\mathbf{w}_k)\,|^2}{\gamma_k^{DL}}\right), \tag{10}$$

in which γ_k^{DL} represents the sum of AP-to-UE interference, IUI and the noise:

$$\gamma_k^{DL} = \sum_{\substack{j=1 \\ j\neq k}}^{K} L_j\left|\mathbf{h}_{\mathcal{C}_j,k}^T\ (\mathbf{P}_{\mathcal{C}_j}\mathbf{w}_j)\right|^2 + p_j(1-L_j)\left|h_{k,j}\right|^2 + \sigma_{\text{DL}}^2. \tag{11}$$

Similarly, the EE considers the ratio between the SE of all UEs in DL and the transmit power of APs that compose their clusters. Then, EE for DL is defined as follows:

$$EE^{DL} = \frac{\sum_{j=1}^{K} L_j R_k^{DL}}{\sum_{j=1}^{K} L_j \text{tr}(\mathbf{P}_{\mathcal{C}_j}\mathbf{P}_{\mathcal{C}_j})}. \tag{12}$$

III. Power Control Algorithm

In order to mitigate the CLI effects and improve the SE and the EE, we consider the implementation of a widely explored power allocation approach in the system. This section presents the FPC and the max power (MP) baseline, both used for UEs in UL.

A. Max Power

The MP baseline is the obvious way to set the power, considering the maximum power resource available at the UE, in which:

$$p_k = P_{\text{max}}\ \forall\ k \in \{1, ..., K\} \text{ in UL mode.} \tag{13}$$

This approach aims to provide the best transmit signal but introduces more interference and leads to excessive use of the energy resource.

B. Fractional Power Control

We adopt the FPC scheme from [9]. which partially compensates the PL effect according to a compensation factor $\alpha \in [0, 1]$ and a multiplicative constant p_0, which is a network parameter obtained empirically with the objective of normalizing the power coefficient. Thus, the transmit power (in W) of a UE k is given by:

$$p_k = \min(P_{\text{max}},\ P_0\ \zeta_k^{-\alpha}), \tag{14}$$

in which P_{max} is the maximum transmit power of k and ζ_k considers the LSF between k and its cluster $\mathcal{C}_k$ as follows:

$$\zeta_k = \sqrt{\sum_{a\in\mathcal{C}_k}\beta_{k,a}}. \tag{15}$$

Differently from the formulation in [9], a multi-antenna scenario is not considered, so that the array steering vector in our case is actually a scalar, thus resulting in (15).

Note that interference terms are not considered in (14) because FPC only aims to provide an arbitrary sufficient performance (according to P_0) for each UE with minimal power expenditure, limiting it to the MP in case of a higher value. Thereby, the FPC algorithm is scalable in such D-MIMO networks as the calculation of p_k in (14) depends only on the PL information of UE k, meaning that its computational complexity does not increase with K. Besides, the use of user-centric AP clusters with fixed N yields a computational complexity that does not increase with M.

IV. Numerical Results

This section presents the results from Monte Carlo simulations performing the FPC algorithm in a D-MIMO system with D-TDD against a baseline that uses MP for all UEs in the same setup. We consider a scenario with $K = 30$ UEs and $M = 120$ APs within a square area of side length $L = 1.2$ km. The user-centric clustering is performed based on LSF according to the description in section II with $N = M/K = 4$. We adopt the maximal ratio combining (MRC) and maximal ratio transmission (MRT) as the receive and transmit beamforming vectors, respectively. As for the proportion of users in UL and DL, we vary the UL percentage in $\rho_{UL} \in \{0, 0.25, 0.5, 0.75, 1\}$.

For simplicity, we consider that each realization represents one time resource with its own transmission configuration. The transmission mode of each UE and its respective cluster is assigned randomly per realization considering the ρ_{UL} value. Other relevant parameters are presented in Table I.

TABLE I
SIMULATION PARAMETERS

Parameter	Value
AP height	11.5 m
UE height	1.5 m
Uplink max power	100 mW
Downlink power of each AP	1 W
Bandwidth	10 MHz
Noise power	$\sigma^2_{UL} = \sigma^2_{DL} = -174$ dBm
Shadowing variance (σ^2_{sh})	4 dB
Rician factor mean and variance (μ_k, σ^2_k)	9 and 5
FPC parameters	$P_0 = -10$ dBm, $\alpha = 0.4$

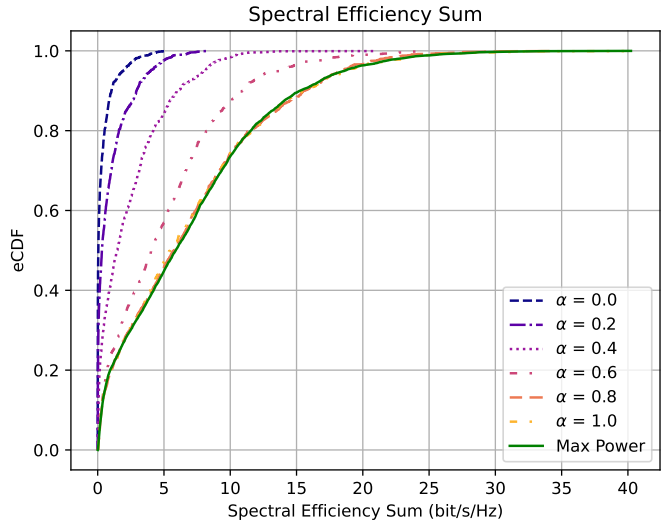

Fig. 2. CDFs of SE varying α FPC parameter.

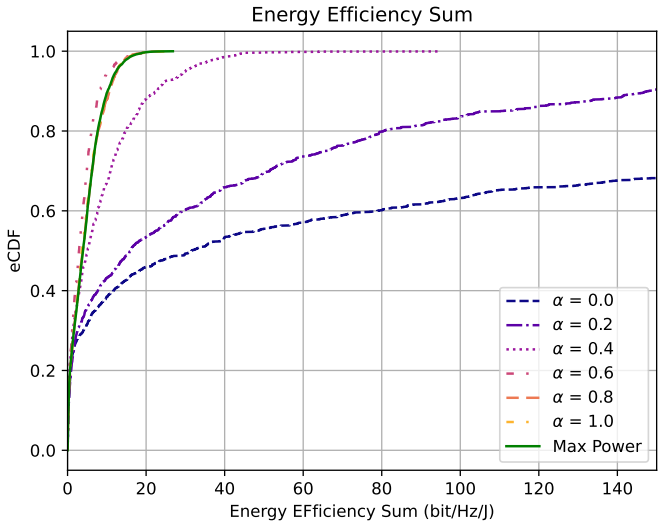

Fig. 3. CDFs of EE varying α FPC parameter.

In both Figs. 2 and 3, we consider a scenario in which FPC is being performed for UEs on UL varying the compensation factor $\alpha \in \{0, 0.2, 0.4, 0.6, 0.8, 1\}$ to determine the best parameter for this scenario. Another scenario is also considered, in which no power control is assumed and MP is set. Here the multiplicative constant is maintained fixed as $P_0 = -10$ dBm.

In Fig. 2, which shows the SE's cumulative distribution function (CDF), we can see that for $\alpha = 0.8$ and $\alpha = 1$, the curves converge to the MP and as the α decreases, the SE also decreases. On the other hand, Fig. 3 shows the EE's CDF and indicates that $\alpha = 0.4$ represents a better EE if compared to lower values of the compensation factor. At the same time, in terms of SE it is closer to the best scenario, which indicates that it is a good trade-off between EE and SE. $\alpha = 0.2$ and $\alpha = 0$ can not be considered because their huge EE values are due to power levels close to 0, which lead to bad SE performance.

Fig. 4 shows the SE's CDF of the following network deployments: (i) MP is set for all UEs in UL, (ii) FPC is applied for all UEs in UL. In both cases, all transmitting APs in DL are set with the same power level and the DL curves represent the UE in DL for each case defined above.

When $\rho_{UL} = 0$ (all UEs are in DL), the SE CDFs for the two nominal schemes are identical. This is because both FPC and MP, as defined, are UL power control strategies, and DL APs maintain a fixed transmission power. For $\rho_{UL} = 0.25$ and $\rho_{UL} = 0.5$, UEs in DL overperform UEs in UL, a trend which changes in $\rho_{UL} = 0.75$ due to the reduction in IAI, that affects UL connections, and the increase in IUI, that affects DL connections. With the exception of the first, in all cases we can see that UEs in UL using FPC consistently exhibit lower SE compared to those using MP. With a minor impact than UL, in DL there is a performance improvement when FPC is applied to the system, which can be seen in the case with $\rho_{UL} = 0.75$.

Fig. 5 shows EE's CDF in the same network deployments as in Fig. 4. Consistently, DL UEs show lower EE compared to UL UEs. This is primarily attributed to the significantly higher transmission power of APs (e.g., 1 W, as per Table I) relative to the maximum UL UE transmission power (100 mW). As the proportion of UL UEs (ρ_{UL}) increases, the EE CDFs for UL UEs shift to the right, indicating improved EE. Notably, FPC consistently yields better EE for UL UEs compared to MP, and this performance advantage for FPC appears to become more significant as ρ_{UL} increases.

V. CONCLUSIONS

This paper aimed to investigate the efficacy of the classical power control approach FPC in enhancing the performance of D-MIMO setups with D-TDD, particularly considering the challenges posed by CLI. We considered that UE-UE channel coefficients follow a Rayleigh distribution, while UE-AP and AP-AP ones follow a Rician distribution. The signal model was described considering the CLI, i.e., the IAI and the IUI, based on which expressions for SE and EE could be presented. The FPC was described in this D-MIMO D-DTDD setup and considerations were made about how it deals with interference. In the numerical results, we showed that the network proportion of UEs in UL and DL influences directly the performance of the users in the respective mode. In other words, if there are more UL UEs than DL UEs, those UEs will tend to

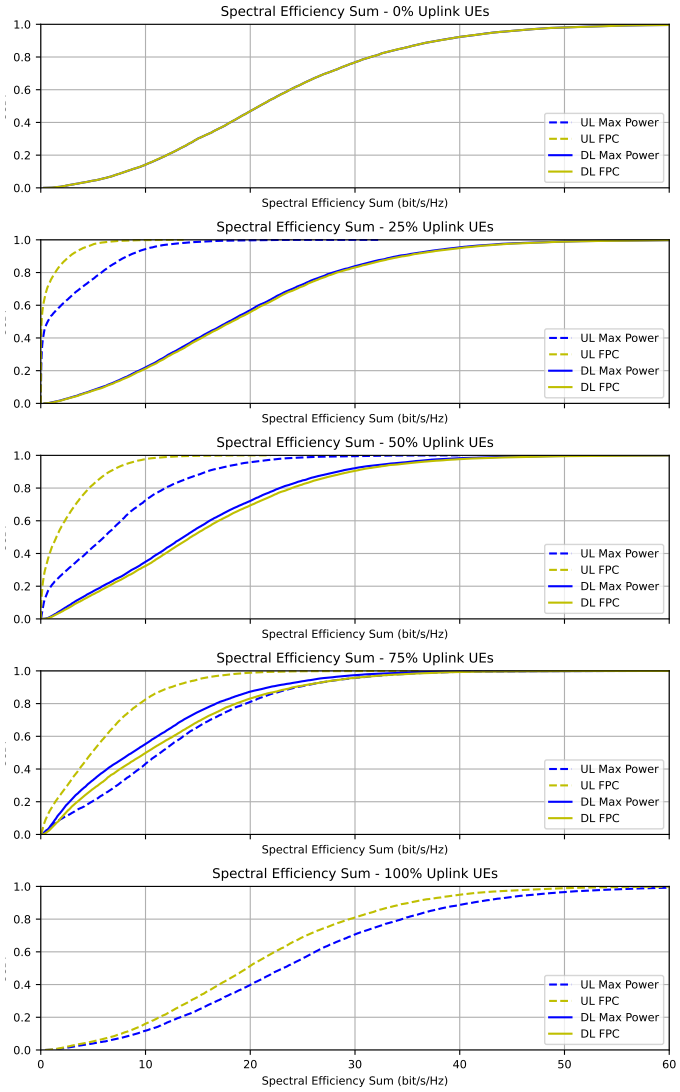

Fig. 4. CDF of UEs SE in UL and DL varying ρ_{UL}.

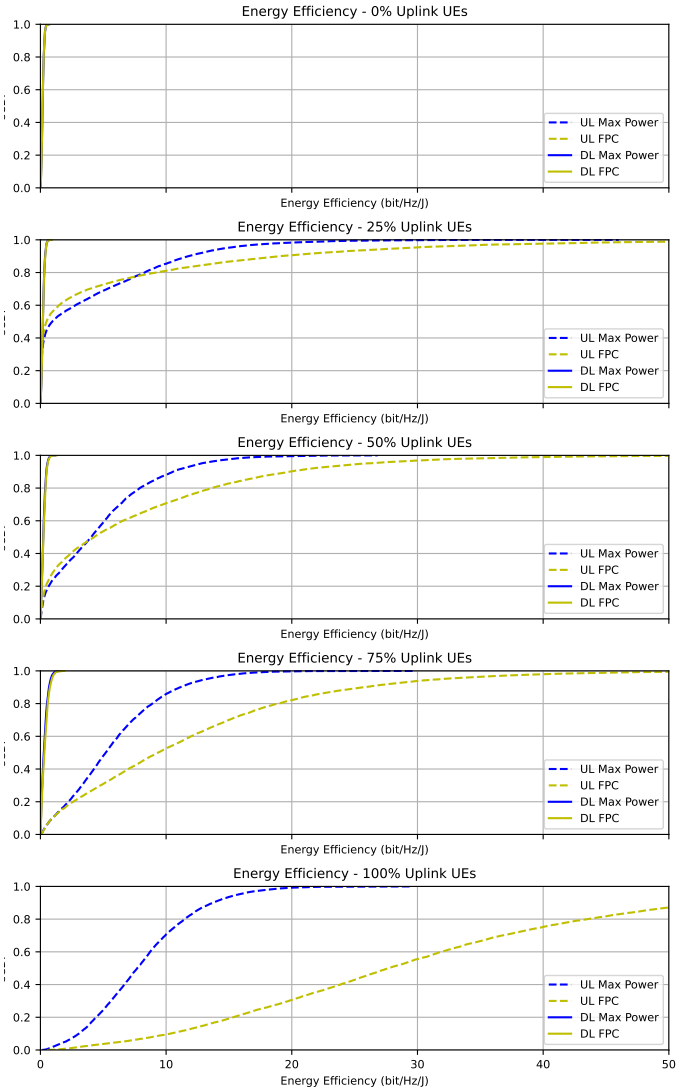

Fig. 5. CDF of UEs EE in UL and DL varying ρ_{UL}.

improve their KPIs, the same for DL. Moreover, we showed that FPC is worse than MP in SE terms but outperforms it when it comes to EE. This indicates that FPC presents a good alternative for optimizing the energy consumption in the upcoming 6G systems, providing a sustainable network operation and a better user experience.

For future works, one may explore DL power allocation algorithms, adopt imperfect channel estimation for robustness analysis, and consider multi-antenna technology to improve system capacity and interference management.

REFERENCES

[1] Özlem Tuğfe Demir, Emil Björnson and Luca Sanguinetti (2021), "Foundations of User-Centric Cell-Free Massive MIMO", Foundations and Trends® in Signal Processing: Vol. 14, No. 3-4, pp 162–472.

[2] H. Kim, H. Lee, T. Kim and D. Hong, "Cell-Free mMIMO Systems with Dynamic TDD," 2022 IEEE 95th Vehicular Technology Conference: (VTC2022-Spring), Helsinki, Finland, 2022, pp. 1-6.

[3] D. Wang, M. Wang, P. Zhu, J. Li, J. Wang and X. You, "Performance of Network-Assisted Full-Duplex for Cell-Free Massive MIMO," in IEEE Transactions on Communications, vol. 68, no. 3, pp. 1464-1478, March 2020.

[4] M. Andersson, T. T. Vu, P. Frenger, and E. G. Larsson, "Joint optimization of switching point and power control in dynamic TDD cell-free massive MIMO," in 2023 57th Asilomar Conference on Signals, Systems, and Computers, Oct. 2023, pp. 988–992

[5] J Rachad, R. Nasri, Laurent Decreusefond. DYNAMIC-TDD INTERFERENCE TRACTABILITY APPROACHES AND PERFORMANCE ANALYSIS IN MACRO-CELL AND SMALL-CELL DEPLOYMENTS. Annals of Telecommunications - annales des télécommunications, 2020.

[6] R. Nikbakht and A. Lozano, "Uplink Fractional Power Control for Cell-Free Wireless Networks," ICC 2019 - 2019 IEEE International Conference on Communications (ICC), Shanghai, China, 2019, pp. 1-5.

[7] F. R. V. Guimarães, G. Fodor, W. C. Freitas and Y. C. B. Silva, "Pricing-Based Distributed Beamforming for Dynamic Time Division Duplexing Systems," in IEEE Transactions on Vehicular Technology, vol. 67, no. 4, pp. 3145-3157, April 2018.

[8] 3GPP, "Study on channel model for frequencies from 0.5 to 100 ghz," 3rd Generation Partnership Project (3GPP), Technical Report TR 38.901, version v17.0.0, Mar. 2022, Online. Available: https://www.3gpp.org/ftp/Specs/html-info/38901.htm.

[9] C. D'Andrea, A. Garcia-Rodriguez, G. Geraci, L. G. Giordano and S. Buzzi, "Analysis of UAV Communications in Cell-Free Massive MIMO Systems," in IEEE Open Journal of the Communications Society, vol. 1, pp. 133-147, 2020.